# Analysis of Delays in Transcriptional Signaling Networks with Time-Varying Temperature-Dependent Rate Coefficients

Marcella M. Gomez *     Matthew R. Bennett †     Richard M. Murray *

November 26, 2013

## Abstract

This paper provides preliminary work in an aim to fundamentally understand the effects of temperature fluctuations in the dynamics of biological oscillators. Motivated by circadian rhythms, we are interested in understanding how time-varying temperatures might play a role in the properties of biochemical oscillators. This paper investigates time-dependent Arrhenius scaling of biochemical networks with delays. We assume these time-delays arise from a sequence of simpler reactions that can be modeled as an aggregate delay. We focus on a model system, the Goodwin oscillator, in which we use time-varying rate coefficients as a mechanism to understand the possible effects of temperature fluctuations. The emergence of delays from a sequence of reactions can be better understood through the Goodwin model. For a high order system and comparably high reaction rates, one can approximate the large sequence of reactions in the model with a delay, which can be interpreted as the time needed to go through the "queue". Such types of delays can arise in the process of transcription for example. To study how these delays are affected by temperature fluctuations, we take the limit as the order of the system and the mean reaction rates approach infinity with a periodically time-varying rate coefficient and obtain periodically time-varying delays. We show that the limit cycle of the Goodwin oscillator varies only in the limit when the oscillator frequency is much larger than the frequency of temperature oscillations. Otherwise, the instantaneous frequency of the oscillator is dominated by the mean value of the time-varying temperature.

## 1   Introduction

Studying temperature dependence in biochemical networks remains important and, yet, less understood in oscillators. Much related research has come about through the study of circadian rhythms. It is well known that circadian clocks robustly maintain a 24 hr period, typically thought to be entrained by light, as can be seen in a detailed model of the mammalian circadian clock proposed in [6] by Leloup and Goldbeter. Temperature dependence in circadian clocks has been slowly emerging as a topic of interest. Lahiri et al. [5] presents a compelling argument to consider temperature dependence as a strong driving factor in the zebrafish circadian clock but, mainly,

---

*The authors are with the Department of Mechanical Engineering, California Institute of Technology, Pasadena, CA 91107, USA {mgomez,murray}@caltech.edu

†M. R. Bennett is with the Department of Biochemistry and Cell Biology, Rice University, Houston, TX 77005, USA matthew.bennett@rice.edu

past work on time-varying Arrhenius scaled rate constants in oscillators has been seen in the study of temperature compensation of circadian clocks. Current theoretical work utilizes mathematical conditions that minimize sensitivity of the period to changes in temperature to reverse engineer a temperature compensating model. For example, Hong et al. [4] provide a theory for how temperature compensation might work in circadian oscillators which depends on a balance of temperature dependent effects. Takeuchi et al. [12] use a similar concept to determine rate constants in a more detailed model taken from Gonze et al. [3], which is then modified to include temperature dependence. Ruoff et al. [10] use the same method to determine rate constants, as they consider the Goodwin model to study temperature effects. Results for time-varying rate coefficients are found numerically and for a small order system.

In this paper, we investigate how delays in biochemical networks are affected by periodically time-varying temperatures. Incorporating delays in models of biological systems has allowed scientists to simplify models, while maintaining qualitative similarities to experimental data [2,11]. This has allowed researchers to identify key functional components of larger networks. Motivated by circadian oscillators, we identify the correct way of incorporating delays in an Arrhenius scaled biochemical network with periodically time-varying temperature. Specifically, we consider the case where the number of chain chemical reactions approach infinity as the reaction rates, also, approach infinity. In essence, this provides a model for a system with a large number of consecutive chemical reactions happening almost instantaneously. For example, one may consider this a good model for the process of transcription. We analytically determine the effective delays that arise in the open loop system driven by periodically time-varying Arrhenius scaled rate coefficients and find that they are also time-dependent. We characterize the time-varying delays based on properties of the time-varying rate coefficient. Last, we study the limit cycle of the resulting Goodwin model as we close the system with a nonlinearity in feedback.

After closing the loop, we demonstrate through simulation that the frequency of the limit cycle is robust with respect to changes in the frequency or phase of the periodically time-varying rate coefficients. Simulations suggest the frequency of the limit cycle is dominated by the mean of the time-varying rate coefficient.

## 2 Delays in the Goodwin model

We now show how delays in biological systems can be derived from the Goodwin model. Consider the Goodwin oscillator of order $N + 1$,

$$\dot{x}_0 = \frac{1}{1 + x_N^2} - \alpha x_0$$
$$\dot{x}_j = -a(x_j - x_{j-1}) \quad \text{for} \quad j = 1, ..., N. \tag{1}$$

We would like to take the limit as $N \to \infty$ in such a way that $\frac{N}{a}$ remains constant. First, consider the frequency response of the $N$ linear differential equations with input $x_0$ and output $x_N$ [9]. We arrive at

$$H_{x_0 \to x_N} = \frac{a^N}{(s + a)^N} \tag{2}$$

and take the limit of the delay distribution function in the frequency domain,
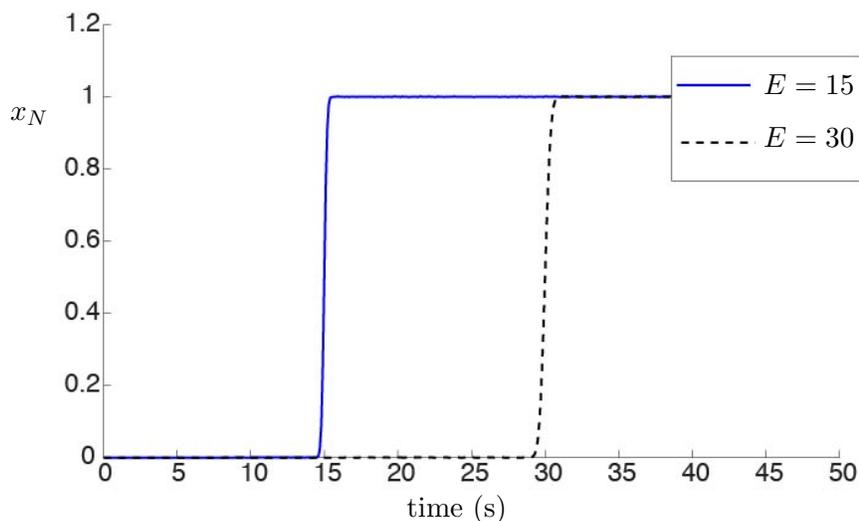
$$\lim_{N \to \infty} H_{x_0 \to x_N}. \tag{3}$$

Figure 1: Open loop simulation with step input for different $E$ and $N = 10,000$.

After rearranging the terms and making substitution $E = N/a$, taking the limit in the frequency domain gives

$$\lim_{N \to \infty} \frac{1}{(\frac{sE}{N} + 1)^{(N)}} = \frac{1}{e^{sE}} = e^{-sE},$$  (4)

which is exactly the frequency response for a delta function $\delta(t - E)$ in the time domain. Therefore, the distribution function will approach a delta function centered at $E$ as $N \to \infty$.

In general, system (1) can be represented as a distributed delay differential equation [7]

$$\dot{x}_0 = \frac{1}{1 + x_N^2} - \alpha x_0,$$

$$x_N = \int_0^\infty h(\tau) x_0(t - \tau) d\tau,$$  (5)

where

$$h(\tau) = \frac{a^N \tau^{N-1}}{(N-1)!} e^{-a\tau}$$  (6)

and $\int_0^\infty h(\tau) d\tau = 1$. Note $E = N/a$ is the mean of the distribution function (6). In the limit as $N \to \infty$, system (1) becomes

$$\dot{x}_0 = \frac{1}{1 + x_0(t - E)^2} - \alpha x_0.$$  (7)

It is worth noting that this specific limit only exists in this framework where all the reaction rates are the same but this simplification helps us to gain insight. In addition, in the limit as $N \to \infty$ the rates must also approach infinity for the distribution to approach a delta function.

We term the mean of the distribution $E = N/a$, the effective delay. Note that for an increased temperature (increased $a$), the effective delay decreases. These results only hold for a constant

3

reaction rate $a$. Figure 1 shows simulations for a unit step input into the open loop system (without the nonlinearity in feedback) for different effective delays. We would now like to investigate how the distribution function changes with a periodically time-varying rate coefficient $a(t)$.

# 3  Delay Distribution Function for Time-Varying Reaction Rates

We investigate the effects of temperature fluctuations on the delay distribution resulting from a sequence of chemical reactions. We begin by considering the following open loop system

$$
\begin{aligned}
\dot{x}_0 &= -a(t)\,x_0 + a(t)\,u(t), \\
\dot{x}_j(t) &= -a(t)(x_j(t) - x_{j-1}(t)) \quad \text{for} \quad j = 1, ..., N.
\end{aligned}
\tag{8}
$$

Note that the reaction rate $a(t)$ is a function of time. Assuming that the rate coefficient's dependence on temperature can be described by the Arrhenius equation of the form

$$
a(t) = Ae^{-E_a/(RT(t))},
$$

oscillations in temperature $T(t)$ will result in oscillations in the rate coefficient $a(t)$. Furthermore, increasing temperature, increases the rate coefficient $a$ as expected. We simplify the model by assuming $a(t)$ is a sinusoidal function with a given period, amplitude, and mean value.

## 3.1  Derivation of the Distribution Function

Now we proceed to find the distribution function in continuous time. We can put system (8) into state space form

$$
\dot{X}(t) = A(t)\,X(t) + B(t)\,u(t)
\tag{9}
$$

with matrices

$$
A(t) = a(t)
\begin{bmatrix}
-1 & 1 & 0 & \dots & 0 \\
0 & -1 & 1 & & \\
\vdots & & \ddots & \ddots & \\
& & & -1 & 1 \\
0 & \dots & & 0 & -1
\end{bmatrix}
\tag{10}
$$

and

$$
B(t) =
\begin{bmatrix}
0 \\
\vdots \\
0 \\
a(t)
\end{bmatrix}.
\tag{11}
$$

Note that $A(t_1)A(t_2) = A(t_2)A(t_1)$ for any $t_1$ and $t_2$. Accordingly, we can write the solution as

$$
X(t) = \exp\left(\int_{t_0}^{t} A(s)\mathrm{d}s\right) X(t_0) + \int_{t_0}^{t} \exp\left(\int_{\tau}^{t} A(s)\mathrm{d}s\right) B(\tau)\,u(\tau)\mathrm{d}\tau.
\tag{12}
$$

We rewrite this expression into a distributed delay format

$$
X(t) = \exp\left(\int_{t_0}^{t} A(s)\mathrm{d}s\right) X(t_0) + \int_{t_0}^{t} \exp\left(\int_{t-\tau}^{t} A(s)\mathrm{d}s\right) B(t - \tau)\,u(t - \tau)\mathrm{d}\tau.
\tag{13}
$$

4

The structure of the system allows for further simplification. Note the Jordan block like structure of the system. With this we find

$$\exp\left(\int_{t-\tau}^{t} A(s)\mathrm{d}s\right) = \exp\left(\int_{t-\tau}^{t} a(s)\mathrm{d}s\, J_{-1,N+1}\right) \tag{14}$$

where $J_{-1,N+1}$ is the $N+1$ Jordan matrix with eigenvalues $-1$. Defining

$$\alpha(\tau) \doteq \int_{t-\tau}^{t} a(s)\mathrm{d}s, \tag{15}$$

the exponential can be computed and is given by

$$e^{\alpha(\tau)J_{-1,N+1}} = \begin{bmatrix} e^{-\alpha(\tau)} & \alpha(\tau)e^{-\alpha(\tau)} & \cdots & \frac{\alpha(\tau)^{N-1}}{(N-1)!}e^{-\alpha(\tau)} & \frac{\alpha(\tau)^{N}}{N!}e^{-\alpha(\tau)} \\ & & & & \frac{\alpha(\tau)^{N-1}}{(N-1)!}e^{-\alpha(\tau)} \\ & & \star & & \vdots \\ & & & & \alpha(\tau)e^{-\alpha(\tau)} \\ & & & & e^{-\alpha(\tau)} \end{bmatrix} \tag{16}$$

where $\star$ denotes non-zero entries that are irrelevant due to the structure of $B(t)$ and our desired output. For our desired output we apply from the left $C = [1, 0, \ldots, 0]$, so that

$$h(\tau) = C\, e^{\alpha(\tau)J_{-1,N+1}} B(t-\tau), \tag{17}$$

and only the top right element of the exponential matrix is needed. This gives the delay distribution function

$$h(\tau) = a(t-\tau)\frac{\alpha(\tau)^{N}}{N!}e^{-\alpha(\tau)}. \tag{18}$$

This solution holds for a general $a(t)$, but we would like to investigate a periodically time-varying reaction rate coefficient

$$a(t) = \delta_a \sin(wt + \phi) + a_0. \tag{19}$$

Just as was done for a constant reaction rate $a$, we would like to see what happens as we take the limit as $N \to \infty$ such that $N/a_0$ remains constant for the time-varying $a(t)$ above.

The delay distribution obtained is time dependent. To study how the delay distribution changes with the phase and period of the temperature fluctuations, we consider the shape of the distribution at time $t = 0$. One can interpret the delay distribution as the probability density function of the time it takes to get through the "queue" modeled by a sequence of chemical reactions. Figures 2 and 3 show the distribution functions for different rate coefficients $a(\tau)$ in equation (19). Although the frequency of variation of $a(t)$ in the second figure is unrealistically high, it is interesting to see the shape the distribution takes. Also, note that the behavior as $\phi$ changes is similar to the behavior one would expect as time evolves. This will be demonstrated in a later section.

## 3.2 The Distribution Function in the Limit as $N \to \infty$

We now proceed to take the limits as $N \to \infty$ such that $N/a_0$ remains constant as was considered in the first section. In order to take the limit, we apply Stirling's formula for large $N$, namely

$$N! \approx \sqrt{2\pi N}\left(\frac{N}{e}\right)^{N} \tag{20}$$
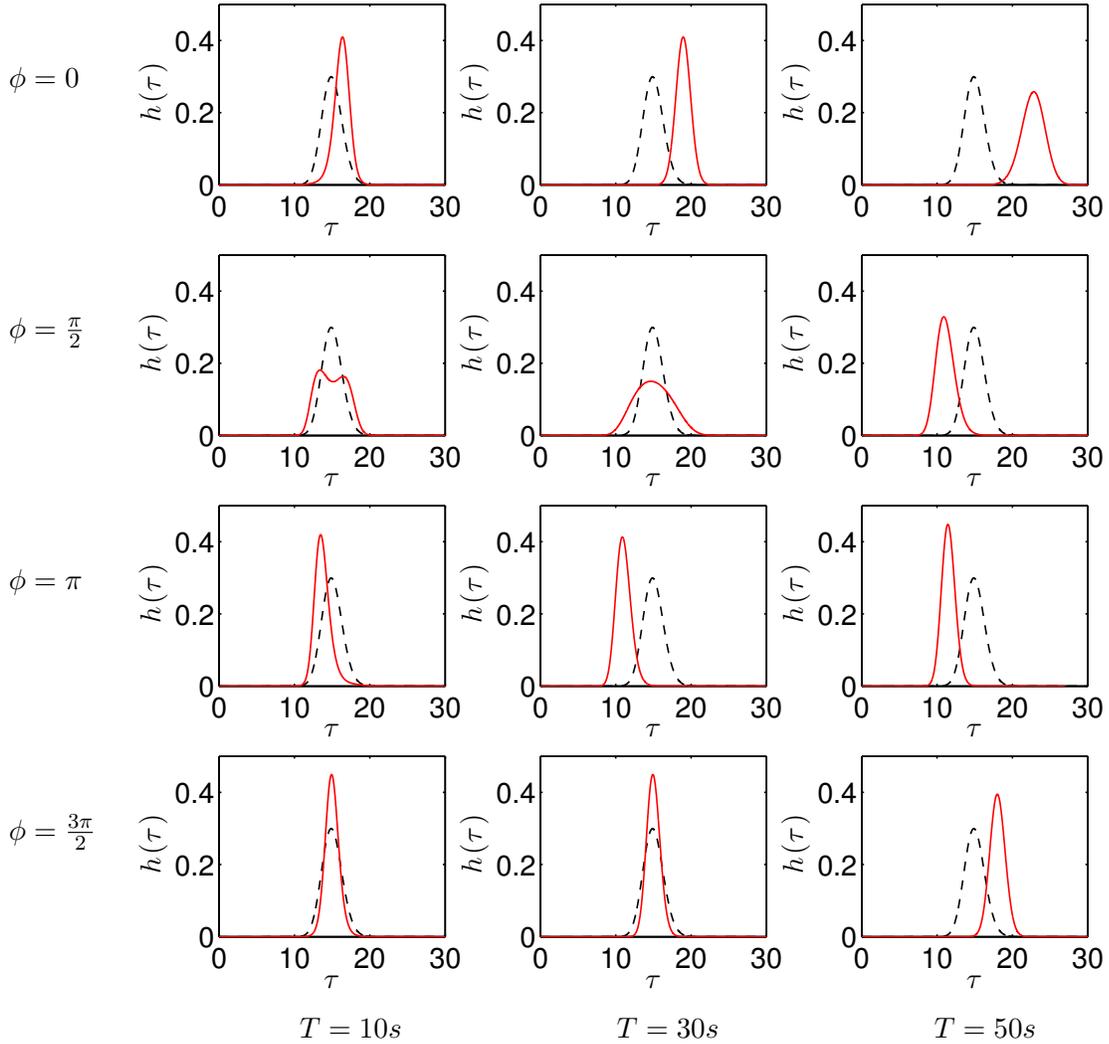
Figure 2: Distribution function for time-varying $a(t)$ (solid line) and constant $a(t) = a_0$ (dashed line) with different periods and phase shifts for $a(t)$ with parameters $a_0 = 8.4$, $\delta_a = .5\,a_0$, $E = 15$, and $N = 125$.
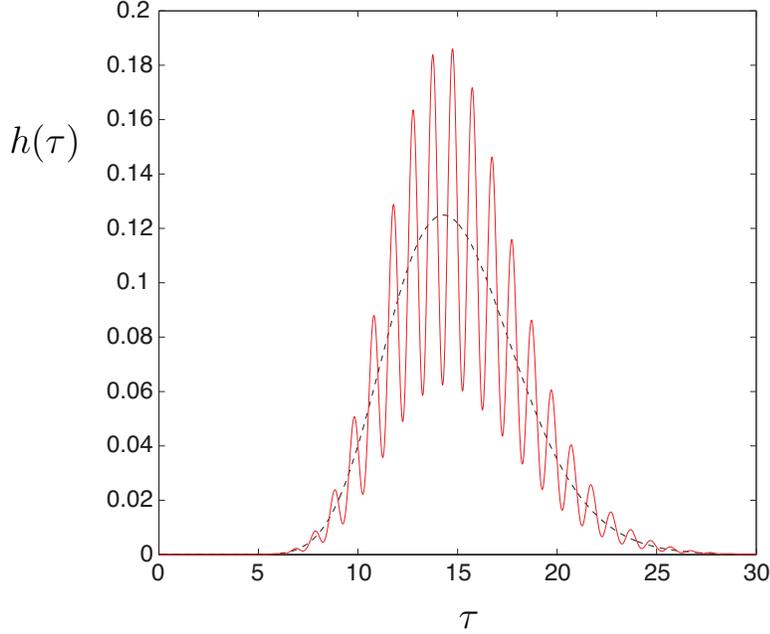
Figure 3: Distribution function for time-varying $a(t)$ (solid line) and constant $a(t) = a_0$ (dashed line) with $T = 1$ and $\phi = 0$ for $a(t)$ with parameters $a_0 = 1.4$, $\delta_a = .5\,a_0$, $E = 15$, and $N = 21$ .

and get

$$h(\tau) = a(t - \tau)\frac{\alpha(\tau)^N}{N!}e^{-\alpha(\tau)} \tag{21}$$

$$\approx \frac{a(t - \tau)}{\sqrt{2\pi N}}\left(\frac{e\,\alpha(\tau)}{N}\right)^N e^{-\alpha(\tau)}. \tag{22}$$

We substitute $a(t - \tau)$ as defined in equation (19) and correspondingly $\alpha(\tau)$ as in equation (15),

$$\alpha(\tau) = \frac{\delta_a}{w}\left[\cos(w(t - \tau) + \phi) - \cos(w\,t + \phi)\right] + a_0\tau. \tag{23}$$

For $N \gg 1$

$$E = \frac{N + 1}{a_0} \approx \frac{N}{a_0}. \tag{24}$$

Rearranging terms in equation (22), after making our substitutions, we get

$$h(\tau) \approx \frac{1}{\sqrt{2\pi E}}\left(\frac{e\,\alpha(\tau)}{N}\right)^N a_0^{\frac{1}{2}}\left(\delta_p\sin(w(t - \tau) + \phi) + 1\right)e^{-\alpha(\tau)} \tag{25}$$

$$\approx \frac{1}{\sqrt{2\pi E}}\left(\frac{e\,\alpha(\tau)}{N}\right)^N\left(\frac{N}{E}\right)^{\frac{1}{2}}\left(\delta_p\sin(w(t - \tau) + \phi) + 1\right)e^{-\alpha(\tau)} \tag{26}$$

$$\approx \frac{1}{\sqrt{2\pi E}}\left(\frac{\alpha(\tau)}{N}e^{1-\alpha(\tau)/N}\right)^N\left(\frac{N}{E}\right)^{\frac{1}{2}}\left(\delta_p\sin(w(t - \tau) + \phi) + 1\right). \tag{27}$$

7

Here $\delta_a = \delta_p a_0$, where $\delta_p$ represents our percent change in $a_0$. Note

$$\frac{\alpha(\tau)}{N} = \frac{\delta_p}{wE} \left[\cos(w(t-\tau)+\phi) - \cos(wt+\phi)\right] + \frac{1}{E}\tau \tag{28}$$

does not depend on $N$ in a way affected by the limit. We define

$$K(\tau) \doteq \frac{\alpha(\tau)}{N} e^{1-\alpha(\tau)/N} \tag{29}$$

and investigate the limit for different ranges of $K$. For $K < 1$

$$\lim_{N\to\infty} \frac{N^{\frac{1}{2}}}{1/K^N} = \lim_{N\to\infty} \frac{\frac{-1}{2}N^{\frac{-1}{2}}}{-N/K^{N+1}} = \lim_{N\to\infty} \frac{K^{N+1}}{2N^{3/2}} = 0 \tag{30}$$

and for $K \geq 1$

$$\lim_{N\to\infty} \frac{N^{\frac{1}{2}}}{1/K^N} = \frac{\infty}{0} = \infty. \tag{31}$$

It remains to show that $K \leq 1$ for all $\tau$. We would like to determine when $K$ reaches its maximum value. As a necessary condition for an extremum we must have

$$\frac{\mathrm{d}}{\mathrm{d}\tau}(K) = \frac{\mathrm{d}}{\mathrm{d}\tau}\left(\frac{\alpha(\tau)}{N}\right) e^{1-\frac{\alpha(\tau)}{N}} \left(1 - \frac{\alpha(\tau)}{N}\right) = 0. \tag{32}$$

Since the first two terms are always strictly positive, we find that an extremum occurs at $\tau_{\text{eff}}$ where

$$1 - \frac{\alpha(\tau_{\text{eff}})}{N} = 0, \tag{33}$$

which can be rewritten as

$$\int_{t-\tau_{\text{eff}}}^{t} \frac{\delta_p}{E}\sin(ws+\phi) + \frac{1}{E}ds = 1. \tag{34}$$

A larger $E$ leads to larger $\tau_{\text{eff}}$ and vice versa. In addition, for increasing $E$ and frequency $w$, one can make the approximation,

$$\tau_{\text{eff}} \approx E$$

alternatively, as $w \to 0$,

$$\tau_{\text{eff}} \approx \frac{E}{\delta_p \sin\phi + 1}.$$

Plugging equation (33) back into equation (29), we note $K = 1$ at the extremum. It can be easily shown that

$$\frac{\mathrm{d}^2}{\mathrm{d}^2\tau}(K) > 0, \tag{35}$$

therefore, the extremum is a maximum. We see that in the limit as $N \to \infty$, $h(\tau)$ is zero everywhere for all $\tau$, except for at $\tau_{\text{eff}}$ when $K(\tau) = 1$, where $h(\tau) = \infty$. It is easy to verify that equation (33) has at minimum a single solution; the solution is the intersection of the line

$$f_1 = 1 - \frac{1}{E}\tau + \frac{\delta_p}{wE}\cos(wt+\phi) \tag{36}$$

and the cosine function

$$f_2 = \frac{\delta_p}{wE}\cos(w(t-\tau)+\phi). \tag{37}$$

It is not as obvious that only one solution exists but this can be shown by applying the mean value theorem [1].

**Theorem 3.1.** *If $f \in C[a, b]$ and $f$ is differentiable on $(a, b)$, then a number $c$ in $(a, b)$ exists with*

$$f'(c) = \frac{f(b) - f(a)}{b - a}.$$

Using the fact that the derivative of $f_2$ is bounded,

$$\frac{\mathrm{d}}{\mathrm{d}\tau} f_2 = \frac{\delta_p}{E} \sin(w(t - \tau) + \phi) \geq -\frac{\delta_p}{E} \tag{38}$$

and the slope of the line $f_1$ is $-1/E$, it holds for all $\tau$ that

$$\frac{\mathrm{d}}{\mathrm{d}\tau} f_1 < \frac{\mathrm{d}}{\mathrm{d}\tau} f_2 \tag{39}$$

for $\delta_p \in (0, 1)$. By consequence of the mean value theorem, there cannot exist two points $f_2(a)$ and $f_2(b)$ connected by a line with slope less than $-\delta_p/E$, hence, $f_1$ cannot intersect more than one point on $f_2$. Therefore, equation (33) is a global maximum and we can make the case that we have a delta function centered at the solution $\tau_{\text{eff}}$ in the limit (we necessarily have $\int_0^\infty h(\tau)\mathrm{d}\tau = 1$). Note that

$$\int_0^\infty h(\tau)\mathrm{d}\tau = \int_0^\infty a(t - \tau)\frac{\alpha(\tau)^N}{N!}e^{-\alpha(\tau)}\mathrm{d}\tau = \int_C \frac{\alpha^N}{N!}e^{-\alpha}\mathrm{d}\alpha, \tag{40}$$

where the last integral is a path integral along the curve $\alpha(\tau)$. The curve $\alpha(\tau)$ is a periodic function that oscillates about a linear function of $\tau$. We have $\alpha(\tau)$ is an injective function $(\mathrm{d}\alpha(\tau)/\mathrm{d}\tau = a(t - \tau) > 0)$ with $\alpha(0) = 0$ and $\alpha(\infty) = \infty$. Therefore, the path integral must equal one.

We investigate how the effective delay $\tau_{\text{eff}}$ changes with time. We define $\tilde{\phi}(t) = w\,t + \phi$ and note that the effective delay is a function of time and periodic with the same frequency $w$ as that of the rate coefficient. Plots of $\tau_{\text{eff}}$ are shown as a function of time in Fig. 4 for different $\phi$. Figure 5 shows simulations for the open loop system (8) with an applied step input at time $t = 0$ for different $\tilde{\phi}$ with $N = 10,000$. The delay in the step response should correspond to the triangular markers in Fig. 4. The triangular makers indicate when the delay is equal to the time that has passed since the step input was applied at $t = 0$.

The plots in Fig 6 show $\tau_{\text{eff}}$ as a function of frequency of $a(t)$ at time $t = 0$. Recall that, as time evolves, each point on the curves in Fig 6 varies periodically. In order to characterize the time-dependent delay as a function of the parameters of $a(t)$, the average value and peak-to-peak amplitude of $\tau_{\text{eff}}$ is plotted against parameters $\delta_p$, $E$, and $w$(Hz) in Fig. 7.

## 4    Closed-Loop System

We now close the open loop system (8) with a nonlinearity in negative feedback

$$u = \frac{1}{1 + (x_N/K_x)^2}, \tag{41}$$

where we choose $K_x = .1$ to ensure oscillations. The closed loop system is then given by

$$\dot{x}_0 = a(t)\, x_0 + a(t)\, \frac{1}{1 + (\tilde{x}_0/K_x)^2}$$

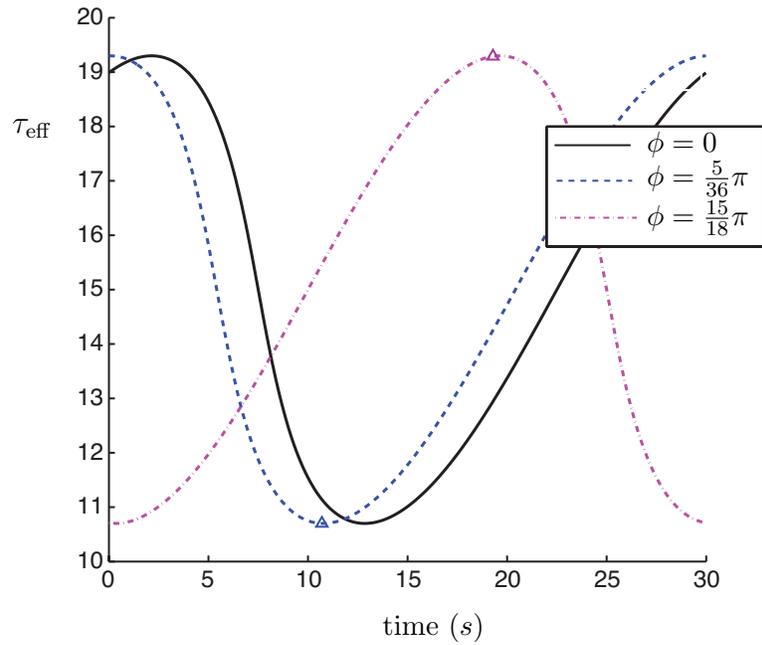$$\tilde{x}_0 = \int_0^\infty h(\tau)x_0(t - \tau)\mathrm{d}\tau. \tag{42}$$

9

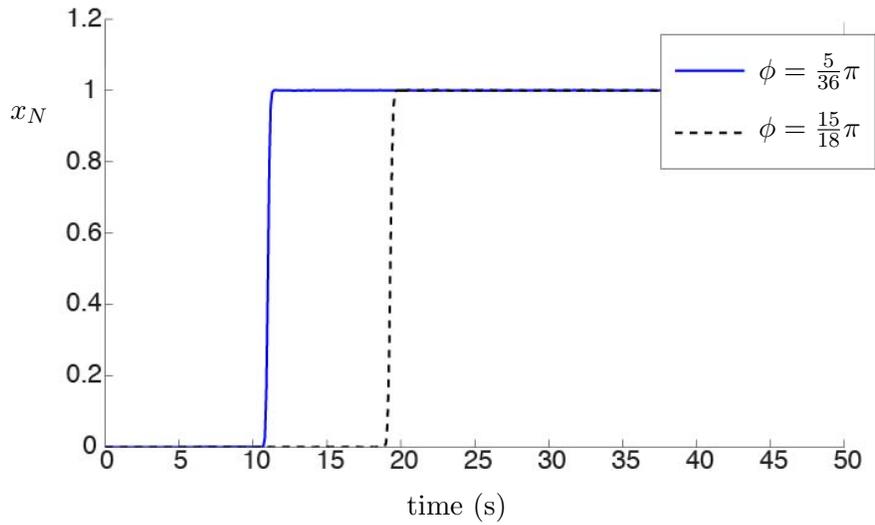Figure 4: $\tau_{\text{eff}}$ as a function of time with constants $\delta_p = .5$, $E = 15$ and $w = \pi/E$.



Figure 5: Open loop simulation with step input for different $\phi$ for $N = 10,000$, $\delta_p = .5$, $w = \pi/E$, and $E = 15$.
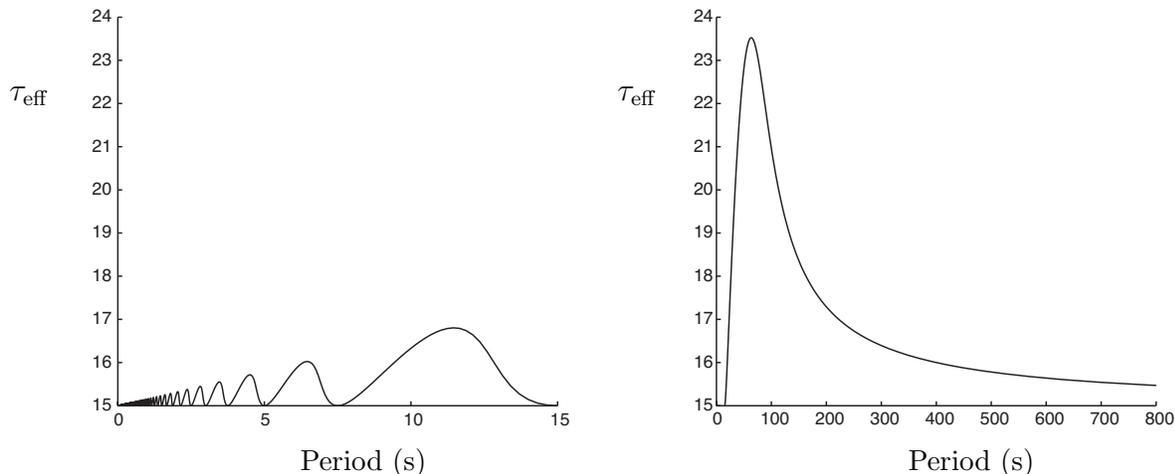
Figure 6: $\tau_{\text{eff}}$ as a function of period of $a(t)$ at $t = 0$ with constants $\delta_p = .5$, $E = 15$ and $\phi = 0$. Left: Plot for period values less than or equal to 15. Right: Plot for period values larger that 15.

In the limit as $N \to \infty$ with $N/a_0$ constant we have

$$\dot{x}_0 = a(t)\, x_0 + a(t) \frac{1}{1 + \left( \frac{x_0(t-\tau(t))}{K_x} \right)^2} \tag{43}$$

where $\tau(t)$ is periodically time-varying delay.

Let us return to the Goodwin model with a constant rate coefficient. The describing function method allows us to approximate the frequency and amplitude of the resulting limit cycle, should a limit cycle exist. See [8] for a more detailed description on harmonic balancing and the describing function method. The frequency of the limit cycle depends only on the linear part of the system, while the nonlinearity determines the amplitude of the limit cycle. Using the describing function method the predicted frequency of the presumed limit cycle is

$$\omega = a_0 \tan \left( \frac{\pi}{N+1} \right) \tag{44}$$

with the period $T = \frac{2\pi}{\omega}$. This is assuming the nonlinearity gives rise to a limit cycle. For $N \gg 1$ we have the approximation

$$\omega \approx a_0 \frac{\pi}{N+1} \tag{45}$$

which gives

$$T \approx 2\, E. \tag{46}$$

Equality holds in the limit as the distribution function approaches a delta function.

For the time-varying $a(t)$ it is interesting to note that we still obtain a delta function in the limit, however, it is no longer necessarily centered at $E = \frac{N+1}{a_0}$ but oscillates around it with a frequency determined by the frequency of the temperature fluctuations and amplitude determined by the relative size of the perturbation and possibly frequency as indicated in Fig. 7. For small
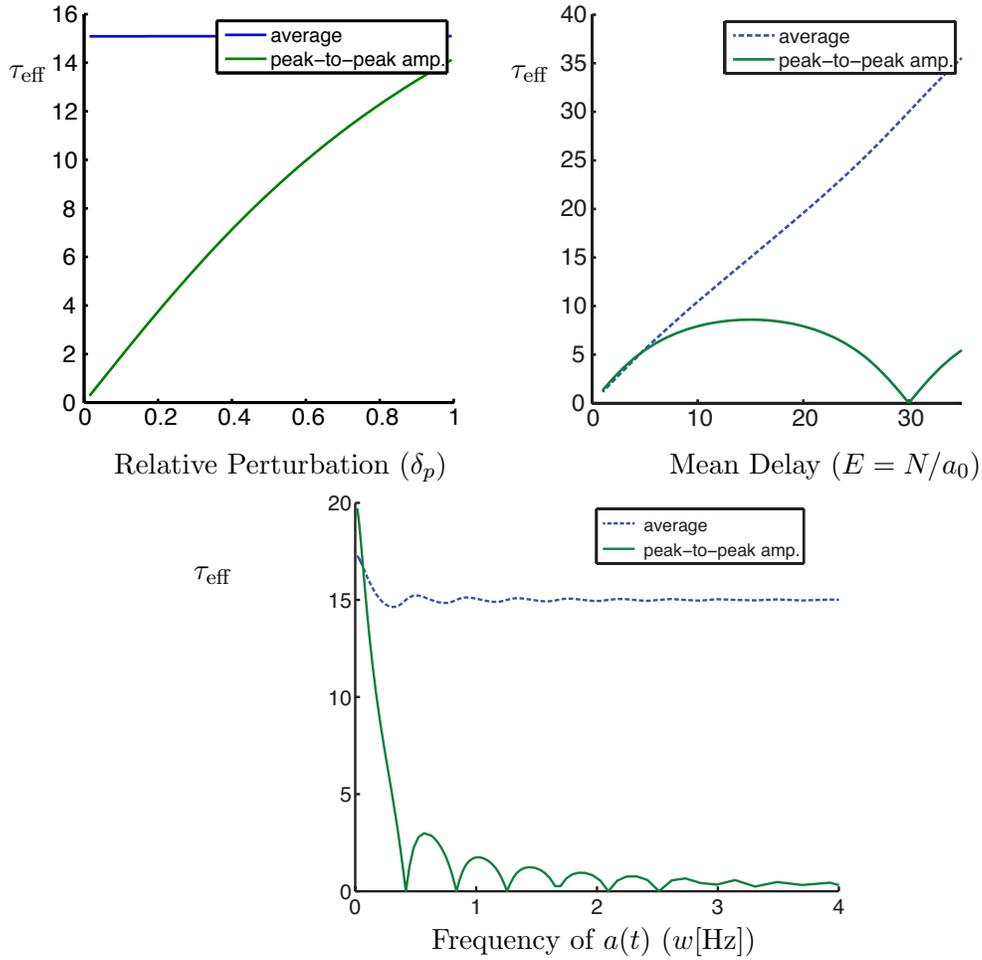
Figure 7: Mean and peak-to-peak amplitude of $\tau_{\text{eff}}$ as a function of $\delta_p$, $E$ and $w$. Top Left: $w = \pi/E$, $\phi = 0$ and $E = 15$. Top Right: $w = \pi/15$, $\phi = 0$ and $\delta_p = .5$. Bottom: $\phi = 0$, $E = 15$ and $\delta_p = .5$
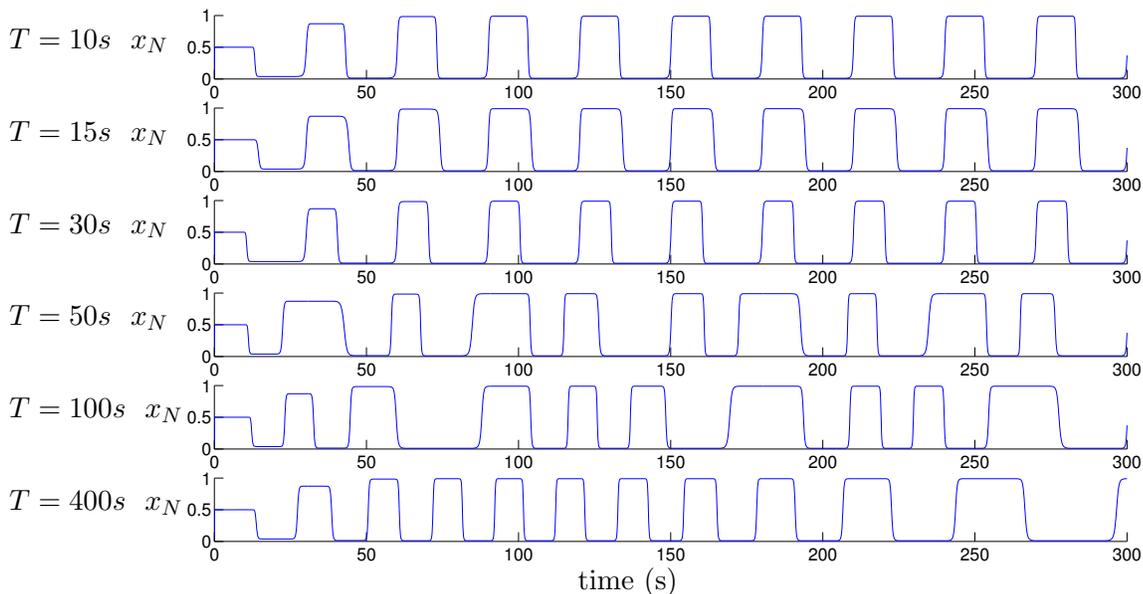
Figure 8: Simulations for different $w$ with constants $\delta_p = .5$, $E = 15$ and $\phi = 0$.

perturbations, one would expect the limit cycle to have a frequency close to that of the nominal system with $a(t) = a_0$. We choose a relatively large perturbation of $\delta_p = .5$ and investigate how the limit cycle changes as the period of $a(t)$ increases. Figure 8 shows simulations of the closed loop system for $N = 10,000$ and $E = 15$ for varying periods of $a(t)$. It is apparent that the period of the limit cycle is robust to oscillatory fluctuations in $a(t)$. The period remains close to $2E$ for a large range of frequencies $w$. As the period gets really large, there is an apparent change in the frequency of the limit cycle over time. There is a higher frequency at high temperatures and a lower frequency at decreasing temperatures. This gives a limit cycle whose frequency appears to also be periodically changing with time.

This is further investigated in Fig. 9. The time span of the last simulation in Fig. 8 is extended and analyzed further. The middle plot in Fig. 9 shows $\tau_{\text{eff}}$ as a function of time for $T = 400s$ and the bottom plot shows the single-sided amplitude spectrum of $x_N(t)$ obtained by taking the fast Fourier transform of the signal. The vertical lines indicate the frequencies corresponding to the period of the limit cycle we would expect given a constant delay at the minimum and maximum values achieved by $\tau_{\text{eff}}$

Next, we investigate whether there occurs entrainment with a change is phase. As was shown, different phases $\phi$ for $a(t)$ lead to changes in the effective delay. We investigate the effects on the phase of the output $x_N$ of the closed loop system. Just as circadian clocks experience a phase shift when we overcome jet lag, we investigate whether there is a similar effect with temperature, namely, is there entrainment. If the period changes even slightly, there is a phase shift that changes linearly as a function of time, however, there is also an initial phase shift due to the change in $\tau_{\text{eff}}$. As the reactions approach a delta function, we can imagine that if we go from $a(t) = a_0$ to time-varying $a(t)$ at $t = 0$, we essentially change the delay in the loop, effectively adding

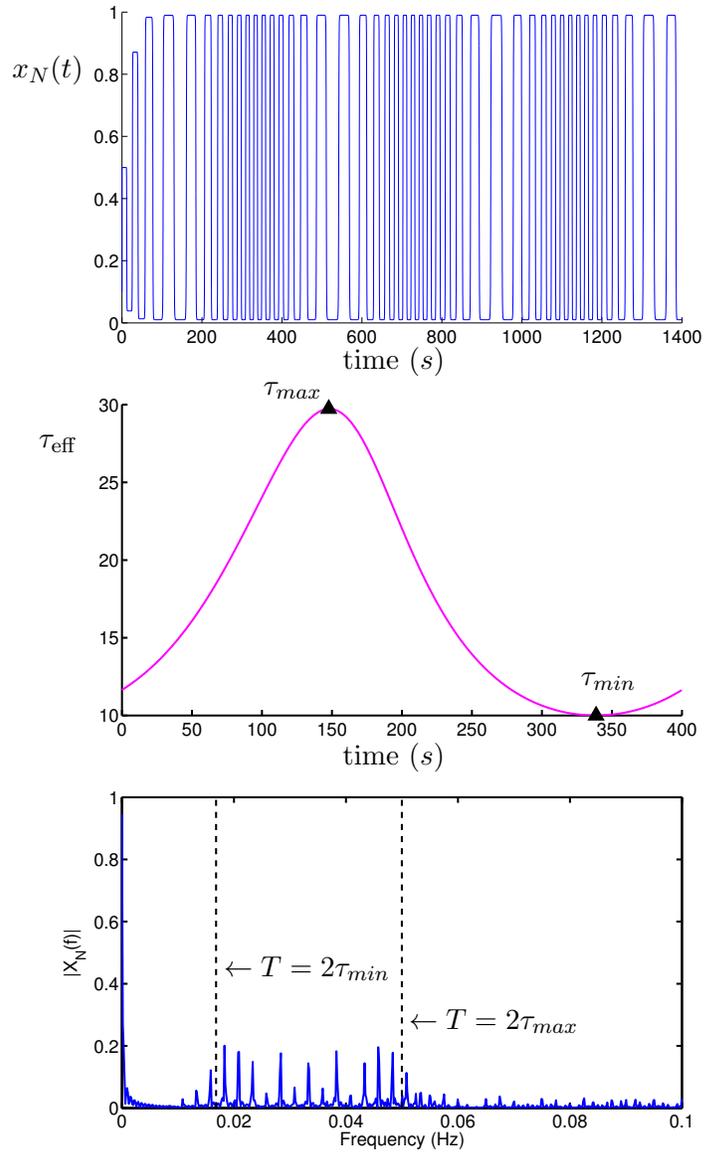$$e^{-s(\tau_{\text{eff}}(0) - E)}$$

13

Figure 9: Top: Extended simulation from Fig. 8 with $T = 400$. Middle: $\tau_{\text{eff}}$ as a function of time. Bottom: Single-sided amplitude spectrum of $x_N(t)$
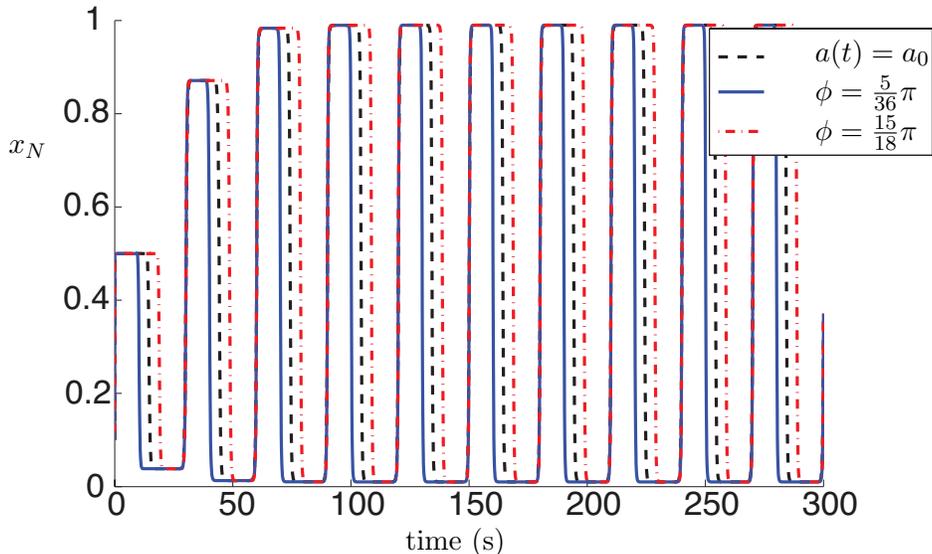
Figure 10: Simulations for different $\phi$ with constants $\delta_p = .5$, $E = 15$ and $w = \pi/E$.

with associated phase $-w(\tau_{\text{eff}}(0) - E)$ in radians, which we expect to be the phase change. A positive term in the exponential does not make sense on its own since that would assume we have information of future states (no longer a delay) but in this case it is reasonable because when added to $e^{-sE}$ it remains a delay, just a smaller delay. Figure 10 shows simulations for different phase shifts $\phi$. The shift in the fall of the signal corresponds to the predicted phase shift but because the width of oscillations change, the actual change in phase is much smaller. In this case, the phase shift seems to be cut by half of what is predicted and the frequency of oscillations remain fairly robust to phase shifts.

## 5    Conclusion

We have shown how delays in chemical reaction networks are affected by periodically driven rate coefficients, particularly, in the Goodwin model. Ultimately we would like to understand how temperature comes into play in circadian oscillators. The periodically time-varying rate functions model temperature fluctuations which are correlated with time of day. It was found that periodic temperature fluctuations induce periodically time-varying delays. In the closed loop, the period of the limit cycle is most strongly influenced by the average value of the rate coefficient. The mean temperature changes from day-to-day and even more drastically from season to season. We have shown robustness of the period with respect to temperature fluctuations. Next, we would like to investigate mechanisms by which an oscillator may be robust to changes in the mean temperature using a delay-based model of a circadian oscillator. In contrast to simply tuning rate constants to get temperature compensation, we would like to explore more fundamental designs that give way to such properties.

# References

[1] Richard L. Burden and J. Douglas Faires. *Numerical Analysis.* Cengage Learning, 9 edition, 2010.

[2] Tal Danino, Octavio Mondragon Palomino, Lev Tsimring, and Jeff Hasty. A synchronized quorum of genetic clocks. *Nature*, 463:326–330, January 2010.

[3] Didier Gonze, José Halloy, and Albert Goldbeter. Robustness of circadian rhythms with respect to molecular noise. *Proc. Natl. Acad. Sci. U.S.A.*, 99(2):673–678, January 2002.

[4] Christian I. Hong, Emery D. Conrad, and John J. Tyson. A proposal for robust temperature compensation of circadian rhythms. *Proc. Natl. Acad. Sci. U.S.A.*, 104(4), 2007.

[5] Kajori Lahiri, Daniela Vallone, Srinivas Babu Gondi, Cristina Santoriello, Thomas Dickmeis, and Nicholas S. Foulkes. Temperature regulates transcription in the zebrafish circadian clock. *PLoS Biology*, 3(11):2005–2016, November 2005.

[6] Jean-Christophe Leloup and Albert Goldbeter. Towards a detailed computation model for the mammalian circadian clock. *Proc. Natl. Acad. Sci. U.S.A.*, 100(12):7051–7056, June 2003.

[7] N. MacDonald. Time lag in a model of a biochemical reaction sequence with product inhibition. *Journal of Theoretical Biology*, 67(3):549–556, August 1977.

[8] A.I. Mees. *Dynamics of Feedback Systems.* John Wiley and Sons, 1981.

[9] Karl J. Åström and Richard M. Murray. *Feedback Systems: An Introduction for Scientist and Engineers.* Princeton University Press, 2008.

[10] Peter Ruoff and Ludger Rensing. The temperature-compensated goodwin model simulates many circadian clock properties. *Journal of Theoretical Biology*, 179:275–285, 1996.

[11] Paul Smolen, Douglas A. Baxter, and John H. Byrne. A reduced model clarifies the role of feedback loops and time delays in the *Drosophila* circadian oscillator. *Biophysical Journal*, 83:2349–2359, November 2002.

[12] Tsutomu Takeuchi, Takamichi Hinohara, Gen Hurosawa, and Kenko Uchida. A temperature-compensated model for circadian rhythms that can be entrained by temperature cycles. *Journal of Theoretical Biology*, 246(1):195–204, May 2007.